DOI: 10.1002/bkcs.12908

PERSONAL ACCOUNT



Check for updates



Stretchable conducting polymer PEDOT:PSS treated with hard-cation-soft-anion ionic liquid designed from molecular modeling

¹Department of Energy Science and Engineering, DGIST, Daegu, Korea

²GREMAN, CNRS UMR 7347, Université de Tours, INSA CVL, Tours, France

³LPS, CNRS UMR 8502, Université Paris-Saclay, Orsay, France

Correspondence

Yun Hee Jang, Department of Energy Science and Engineering, DGIST, Daegu 42988, Korea. Email: yhjang@dgist.ac.kr

Abstract

PEDOT:PSS, an ionic polymer mixture of positively-charged poly-3,4ethylenedioxythiophene (PEDOT⁺) and negatively-charged poly-styrenesulfonate (PSS⁻), is a water-processable and environmentally-benign organic semiconductor and electrochemical transistor, which plays a key role in organic (bio)electronic devices. However, pristine PEDOT:PSS films form 10-to-30-nm granular domains, where conducting-but-hydrophobic PEDOT-rich cores are surrounded by hydrophilic-but-insulating PSS-rich shells. Such morphology makes PEDOT:PSS water-soluble and thermally stable but very poor in conductivity. A tremendous amount of effort has been made to enhance the conductivity of PEDOT:PSS by restoring the extended conduction network of PEDOT. Recently, remarkable ~5000-fold improvements of conductivity have been achieved by mixing PEDOT:PSS with proper ionic liquids (ILs). In a series of free energy estimations using density functional theory calculation and molecular dynamics simulation, we have demonstrated that the classic hard-soft acid-base (or cation-anion) principle of chemistry plays an important role in such improvements. Ion exchange between PEDOT+:PSS- and A+:X- ILs helps PEDOT+ to decouple from PSS⁻ and to grow into large-scale conducting domains of π -stacked PEDOT⁺ decorated by IL anions X⁻. Thus, the most spontaneous decoupling between soft (hydrophobic) PEDOT⁺ and hard (hydrophilic) PSS⁻ would be induced by strong interaction with soft anions X⁻ and hard cations A⁺, respectively. Such hard-cation-soft-anion principles have led us to design ILs containing extremely hydrophilic (i.e., protic) cations and hydrophobic anions. Not only they indeed improve the conductivity of PEDOT:PSS but also enhance its stretchability as well. In summary, our modeling offered molecular-level insights on the morphological, electrical, and mechanical properties of PEDOT:PSS and a molecular-interaction-based enhancement strategy for intrinsically stretchable conductive polymers.

KEYWORDS

conductivity, density functional theory, hardness, hydrophilicity, ion exchange free energy, ionic conducting polymer, ionic liquid, molecular dynamics simulation, morphology, PEDOT:PSS, stretchability

This is an open access article under the terms of the Creative Commons Attribution-NonCommercial-NoDerivs License, which permits use and distribution in any medium. provided the original work is properly cited, the use is non-commercial and no modifications or adaptations are made. © 2024 The Author(s). Bulletin of the Korean Chemical Society published by Korean Chemical Society and Wiley-VCH GmbH.

12295949, 2024, 11, Downloaded from https://onlinelibrary.wiley.com/doi/10.1002bkcs.12908 by Daegu Gyeongbuk Institute Of, Wiley Online Library on [23/12/2024]. See the Terms and Conditions (https://onlinelibrary.wiley.com/term

onditions) on Wiley Online Library for rules of use; OA articles are governed by the applicable Creative Commons

INTRODUCTION

Materials is so important in civilization that the human history is often defined by materials: the stone age, the bronze age, the iron age, and then the polymer-plastic age (Figure 1). What about now? Since the invention of the transistor in 1948,²⁻⁴ we are surrounded by all kinds of electronic devices containing silicon semiconductors. No one would deny that we now live in the silicon age. 1

A conducting polymer with π conjugation along alternating single-double bonds of its backbone was discovered in 1977. The flexibility of such organic semiconductors or synthetic metals is a critical feature for realizing foldable phones and roll-able TVs as well as artificial skin and retina and other biomedical implants (Figure 1),⁵⁻⁹ especially when they are thermoelectric or piezoelectric as well. Organic soft (bio)electronic devices using them are slowly replacing or complementing silicon-based hard electronic devices. Wearable devices such as a smart watch will soon be replaced by skin-like patch devices, which can even go inside our body to correct irregular heartbeats or improve our brain functions (Figure 1). 10-14 We are now entering the renaissance of the polymer age.

PEDOT:PSS, a key player in bioelectronics

Currently, one of the key players in bioelectronics is PEDOT:PSS polymer (Figure 2),5-11 which is an ionic mixture of positively-doped conductive poly-3,-4-ethylenedioxythiophene (PEDOT⁺)¹⁶⁻¹⁸ and negativelycharged insulating poly-styrenesulfonate (PSS⁻).¹⁸⁻²⁰ This ionic conducting polymer or conducting polyelectrolyte has been used to realize transparent, lightweight, flexible, and thus printable and mass-producible electronic/ electrochemical devices, such as organic transistor, light emitting diode, solar cell, sensor-actuator, thermoelectric generator, and ultimately artificial skins. 5-11,20-26 PEDOT:PSS is also water-processable and thus relatively biocompatible and environmentally-benign. However, even this state-ofthe-art organic semiconductor shows a significantly lower electrical conductivity than its inorganic counterpart, indium tin oxide (ITO). This is surprising because vapordeposited PEDOT crystals are supposed to show high conductivities (Figure 2, top).²⁷

The conductivities of water-processed PEDOT:PSS films are poor (<10 S cm⁻¹) because two types of ionic polymers of opposite charges and different lengths (PEDOT $^+$ of 6–18 EDOTs and PSS $^-$ of \sim 2000 SS units) are electrostatically bound to form granular domains (Figure 2, middle).²⁸ In each domain of 10-30 nm, a hydrophilic-but-insulating PSS-rich shell surrounds a conducting-but-hydrophobic PEDOT-rich core (Figure 2, middle). This nano-domain morphology makes PEDOT:PSS stable and water-soluble but the absence of an extended conducting network of PEDOT domains results in poor conductivity.^{28–39} Tremendous effort has been



(Bottom) Materials and human history. Adapted from FIGURE 1 reference [1]. (Top) With the advent of soft and stretchable skin-like electronics made of organic semiconductors (references [5-14]), we enter the renaissance of polymer age.

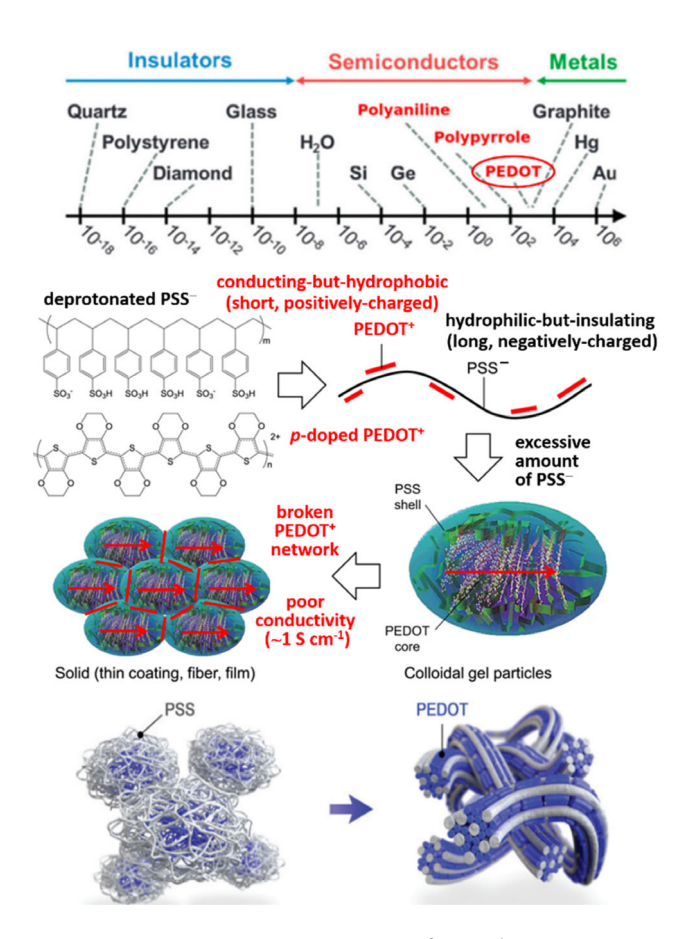


FIGURE 2 (Top) High conductivity ($\sim 10^3$ S cm⁻¹) of vapordeposited PEDOT crystals (reference [27]; copyright RSC 2015). (Middle) Low conductivity (\sim 1 S cm $^{-1}$) of water-processed pristine PEDOT:PSS films (reference [28]; copyright IOP 2014). (Bottom) Various treatments can restore and extend the broken PEDOT networks to improve conductivity (reference [29]; copyright Wiley 2024).

12295949, 2024, 11, Downloaded from https://onlinelibrary.wiley.com/doi/10.1002/bkcs.12908 by Daegu Gyeongbuk Institute Of, Wiley Online Library on [23/12/2024]. See the Terms

ons) on Wiley Online Library for rules of use; OA articles are governed by the applicable Creative Commons

made to enhance the conductivity of PEDOT:PSS by restoring/extending the broken PEDOT conduction networks (Figure 2, bottom). The highest conductivity so far (>4000 S cm $^{-1}$) has been achieved by acid treatments with conc. H_2SO_4 (or more hydrophobic acids CH_3SO_3H , HI, or CF_3SO_3H ; see below), $^{29,32,40-44}$ but these processes exhibit acid-related stability issues. 45 Treating with polar solvents such as ethylene glycol and dimethyl sulfoxide has also improved the conductivity of PEDOT:PSS (≈ 5000 S cm $^{-1}$). $^{46-49}$

lonic liquid treatment for conductive PEDOT:PSS

A remarkable 5000-fold improvement of conductivity up to 2000 S cm⁻¹ has been achieved by a non-acidic treatment, in which an aqueous PEDOT:PSS solution is vigorously mixed with an ionic liquid (IL) composed of 1-ethyl-3-methylimidazolium (EMIM⁺) cations and tetracyanoborate (TCB⁻) anions (Figure 3).^{50,51} Various experiments, such as x-ray photoelectron spectra (XPS) of the S_{2p} levels and transmission electron microscopy (TEM),⁵¹ indicate a mechanism that the best IL pairs, EMIM⁺:TCB⁻, trigger an ion exchange with PEDOT⁺:PSS⁻, decoupling of TCB⁻-bound PEDOT⁺ from EMIM⁺-bound PSS⁻, and finally lead to the growth of large conducting PEDOT⁺ domains decorated by TCB⁻ anions (Figure 3).

Ion exchange free energy (DFT and PMF)

The feasibility of the ion exchange between PEDOT:PSS and IL (e.g., EMIM:TCB) can be judged⁵²⁻⁵⁶ by the aqueous-phase ion-exchange free energy $(\Delta G_{\text{ex.ag}})$ defined as $\Delta G_{aq}(PEDOT^+:TCB^-) + \Delta G_{aq}(EMIM^+:PSS^-)$ – $\Delta G_{ag}(PEDOT^+:PSS^-) - \Delta G_{ag}(EMIM^+:TCB^-)$, i.e., the free energy change during ion exchange in the aqueous phase (Figure 3, bottom). After rearrangement, $\Delta G_{\text{ex,aq}}$ can also be expressed as the change in the agueousphase ion pair binding free energy during the ion exchange, i.e., $\Delta G_b(PEDOT^+:TCB^-) + \Delta G_b(EMIM^+:PSS^-) \Delta G_b(PEDOT^+:PSS^-) - \Delta G_b(EMIM^+:TCB^-)$. To calculate the ion pair (binding) free energies, PEDOT:PSS can be minimally modeled (Figure 4, top) by an EDOT trimer with a unit positive charge (3EDOT⁺)⁵⁷⁻⁶⁰ and a SS monomer with a unit negative charge (SS⁻ or p-toluenesulfonate PTS⁻). The geometry of each ion pair is first optimized in the gas phase, giving the total energy E_q and then verified by a normal mode analysis which gives the zeropoint energy ZPEq and the free energy correction at 298 K, $\Delta\Delta G_{0\to 298 \text{K,g}}$. The gas-phase free energy ΔG_g is obtained as $E_g + \text{ZPE}_g + \Delta\Delta G_{0\to 298 \text{K,g}}$ and then combined to give $\Delta\Delta G_{\text{ex,g}}$ in the gas-phase (Figure 3, bottom right, black dashed curve).⁵² These density functional theory (DFT) calculations were performed with B3LYP/6-31+ +G** using the Jaguar (Schrodinger) code. 61,62 The

calculated $\Delta\Delta G_{\rm ex,g}$ values show a good correlation with the anion dependence of the PEDOT:PSS conductivity enhancement, i.e., more negative $\Delta\Delta G_{\rm ex,g}$ values for the cases of more spontaneous ion exchange and more efficient conductivity enhancement (i.e., EMIM:TCM and EMIM:TCB). However, the anion dependence calculated in the gas phase is exaggerated with a wide range of

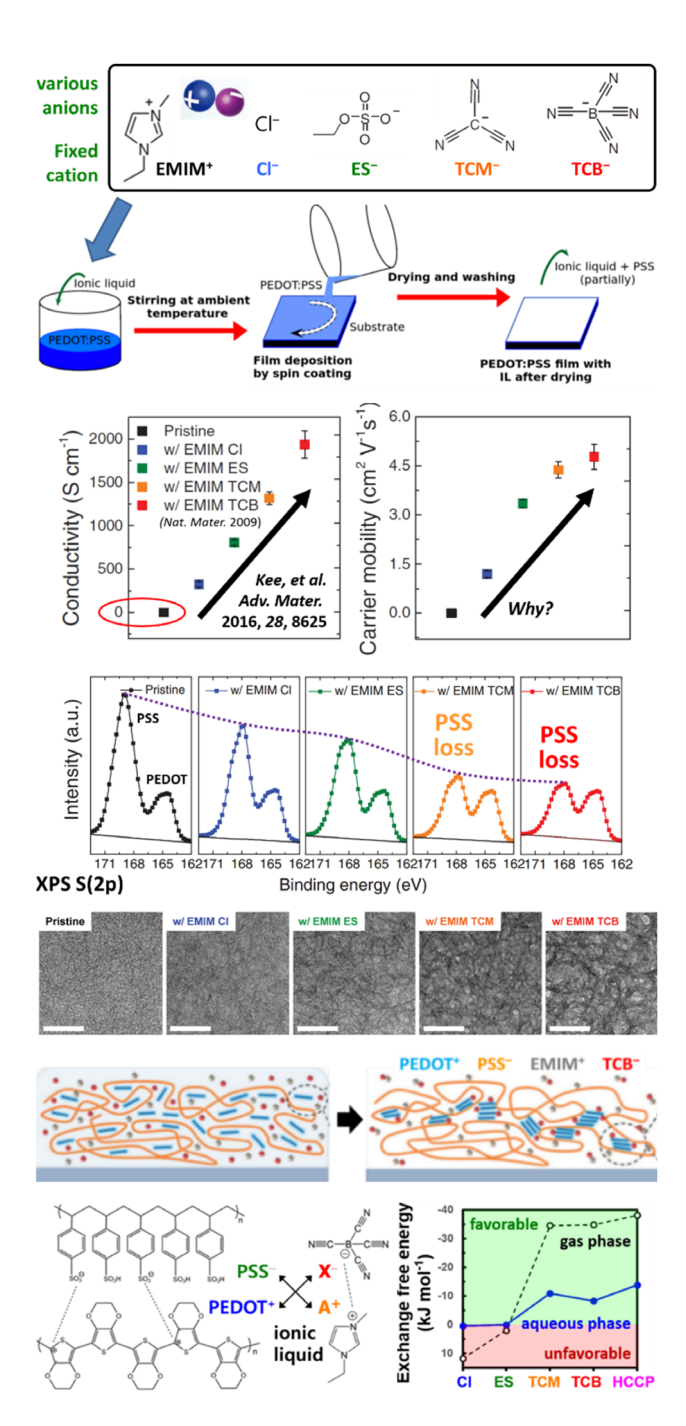


FIGURE 3 (Top) IL treatment of PEDOT:PSS. (Middle) Dramatic IL anion dependence of the enhanced conductivity/mobility. (Bottom) XPS and SEM indicate PEDOT:PSS separation and PEDOT network growth (reference [51]; copyright Wiley 2016) induced by various degrees of ion exchange with IL, confirmed by DFT calculations (references [52–54]; copyright ACS 2018 and 2021).

ditions) on Wiley Online Library for rules of use; OA articles are governed by the applicable Creative Commons

 $\Delta\Delta G_{\rm ex,g}$ (-10 to 40 kJ mol⁻¹).⁵² The anion dependence becomes more reasonable with a narrower range of $\Delta\Delta G_{\rm ex,aq}$ (0 to -10 kJ mol⁻¹; Figure 3, bottom right, blue solid curve)⁵³ when the ion exchange free energy $\Delta\Delta G_{\rm ex,aq}$ is calculated in the aqueous phase by combining the aqueous-phase ion-pair binding free energies ($\Delta G_{\rm b,aq}$) instead of those in the gas phase ($\Delta G_{\rm b,g}$). To estimate the binding energy of each ion pair in the aqueous phase ($\Delta G_{\rm b,aq}$), the DFT-optimized ion-pair geometry was used as the initial geometry of the potential-of-meanforce (PMF) molecular dynamics (MD) simulation running with an umbrella sampling⁶³ along the reaction coordinate ξ , i.e., the distance between the centers of mass (CMs) of cation and anion, in a tetragonal periodic water

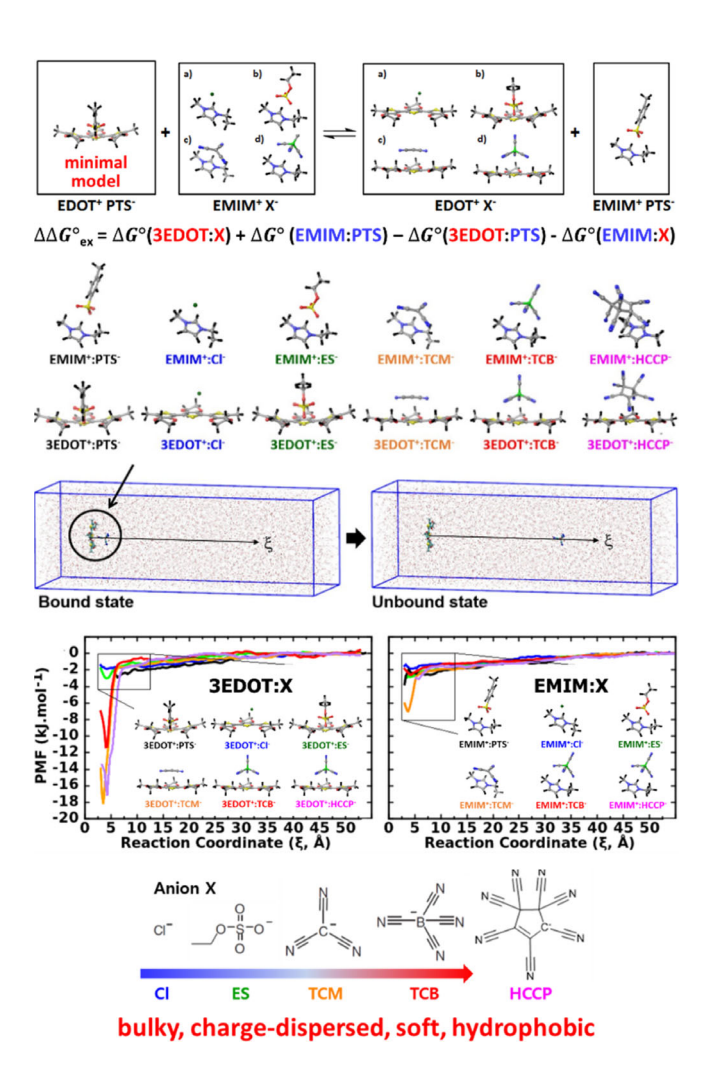


FIGURE 4 (Top) Minimal models for ion exchange between PEDOT:PSS and IL (EMIM:X). (Middle) Monte-Carlo-sampled and DFT-optimized geometries of these minimal models, i.e., 3EDOT:X and EMIM:X (X = PTS, CI, ES, TCM, TCB, and HCCP) ion pairs (reference [52]; copyright ACS 2018). (Bottom) They are used as the initial geometry for PMF simulations along the reaction coordinate ξ , i.e., the CM-CM distance between cation (3EDOT or EMIM) and anion X, in a tetragonal periodic water box of $4\times4\times12$ nm³ (reference [53]; copyright ACS 2021). [Color code: H (black), B (green), C (gray), N (blue), O (red), and Cl (dark green).]

box of $4 \times 4 \times 12 \text{ nm}^3$ containing about 6450 water molecules (Figure 4, bottom).

The anion dependence is less exaggerated in the aqueous phase than in the gas phase, because the ionpair binding energy ΔG_b is less negative (i.e., binding is less strong) in the aqueous phase (e.g., -12 instead of -250 kJ mol^{-1} in case of 3EDOT:TCB) due to stabilization of dissociated individual ions by hydration. 52,53 If the bulkiness, the charge-dispersion, the hardness-softness, and the hydrophilicity-hydrophobicity of an ion is defined by its hydration energy (i.e., the less negative hydration energies and the weaker hydration for the bulkier, more charge-dispersed, softer, and more hydrophobic ions),⁵³ the consistently deeper PMF minima (stronger binding) estimated for 3EDOT:X pairs than for EMIM:X pairs (Figure 4, bottom) indicate that 3EDOT⁺ in PEDOT:PSS is a more hydrophobic (softer) cation than EMIM⁺ in IL. The deeper PMF minima estimated for 3EDOT:TCM and 3EDOT:TCB than for 3EDOT:Cl and 3EDOT:ES (Figure 4, bottom left) likewise indicate that tricyanomethanide TCM⁻ and TCB⁻ are softer and more hydrophobic anions than chloride Cl and ethylene sulfate ES (Figure 4, bottom).

Since the PMF simulation is extremely time-consuming and labor-intensive, such a critical effect of hydration on ion exchange can be taken into account alternatively by reoptimizing the ion-pair geometry in the Poisson–Boltzmann implicit solvation model of water in the frame of DFT^{64,65} and then by adding the estimated hydration free energy $(\Delta G_{\rm hyd})$ to the gas-phase free energy to estimate the aqueous-phase free energy $\Delta G_{\rm aq}$ (= $\Delta G_{\rm g} + \Delta G_{\rm hyd}$) of each ion pair. SI t should be noted that we estimate $\Delta G_{\rm hyd}$ and in turn $\Delta G_{\rm aq}$ of the neutral ion pairs only, not the individual ions, with the implicit solvation models and combine them to estimate the ion-exchange free energy $\Delta \Delta G_{\rm ex,aq}$.

Design principle: Hard-cation-soft-anion IL

We then notice that the classic hard-soft acid-base principle of Pearson^{66–69} plays the central role in the ion exchange between PEDOT:PSS and IL.51-55 The deprotonated PSS⁻, like ES⁻, is a hydrophilic (hard) anion (base) that can form hydrogen (H) bonds with water, and the pdoped PEDOT⁺ is a hydrophobic (soft) cation (acid) that has a single positive charge dispersed over at least three π -conjugated EDOT units. ^{57–60} Therefore, the most favorable ion exchange with PEDOT+:PSS- would be achieved by ILs of the most hydrophobic anion and the most hydrophilic cation. This principle indeed explains the experimental findings that the most hydrophobic anions TCM⁻ and TCB⁻ are favored for the PEDOT:PSS treatment (Figure 3, middle). A hypothetical anion with seven cyano groups attached to a non-planar partially-aromatic central ring, heptacyanocyclopentenide (HCCP⁻), was designed as an extremely bulky and hydrophobic (soft) anion, and

it indeed exhibits the most negative ion exchange free energy among the series of considered anions (Figures 3 and 4).

Mixing IL with aqueous PEDOT:PSS Solution (MD)

Larger-scale MD simulations mimicking the vigorous mixing of IL in the aqueous PEDOT:PSS solution (Figures 2 and 5) also confirm the favorable ion exchange induced by ILs with hydrophobic anions. Larger PEDOT:PSS models, e.g., 48 chains of doublycharged 6-unit oligomer 6EDOT²⁺ and 6 chains of 16-unit fully-deprotonated oligomer 16SS¹⁶⁻, are mixed and equilibrated in a 12-nm periodic cubic box filled with about 54 000 SPC/E water⁷⁰ molecules.^{54,55} A model of an intermediate size, e.g., 16 chains of 3EDOT⁺ and a single chain of 16SS¹⁶⁻ mixed in a 6-nm periodic cubic box of water, are also used for clearer visualization (Figure 5). 52,54,55 The PSS-to-PEDOT weight ratio (3:1) is comparable to 2.5:1 of the CleviosTM PH1000 PEDOT:PSS solution.⁵¹ From the final MD snapshot of the pristine PEDOT:PSS solution, water molecules are randomly chosen and replaced by EMIM:X IL pairs. Interatomic interactions in the system are described by the OPLS-AA-based⁷¹⁻⁷³ force field of Zozoulenko and coworkers^{35,36,74,75} supplemented with electrostatic-potential-fitted atomic charges obtained from the above DFT calculations. 52-55 The particle-mesh Ewald summation^{76,77} implemented in GROMACS^{78,79} handles long-range electrostatic interactions and shortrange electrostatic and van der Waals interactions are truncated at 14 Å. After a short steepest-descent minimization and a 60-ns NVT simulation with the modified Berendsen thermostat⁸⁰ at 293 K, each system is submitted to a simulated annealing run (which linearly increases the temperature from 293 to 363 K during 10-ns NPT run and decreases back to 293 K during 20ns NPT run) at 1 atm to mimic IL mixing conducted in experiments, and finally to a 180-ns NPT simulation at 293 K and 1 atm with the Nose-Hoover thermostat^{81,82} and the Parrinello-Rahman barostat.83,84 A time step of 2 fs is used for the leap-frog integration. 85 Cluster analyses using a friends-of-friends algorithm⁸⁶⁻⁸⁹ and a threshold distance of 3.5 Å retrieve the size and the composition of PEDOT clusters formed before and after mixing PEDOT:PSS with IL pairs (Figure 6).

From the equilibrium structures (the final snapshots) taken after the MD simulations (Figure 5, bottom), we first notice the self-agglomeration of hypothetical EMIM:HCCP ILs, which suggests that they are too hydrophobic to be water soluble. Other ILs used in the previous real experiments⁵¹ indeed exhibit no trace of self-agglomeration, either dispersed in the water phase or deposited on the surface of PEDOT or PSS, confirming their decent water solubility. We also notice that IL-induced PEDOT-PSS

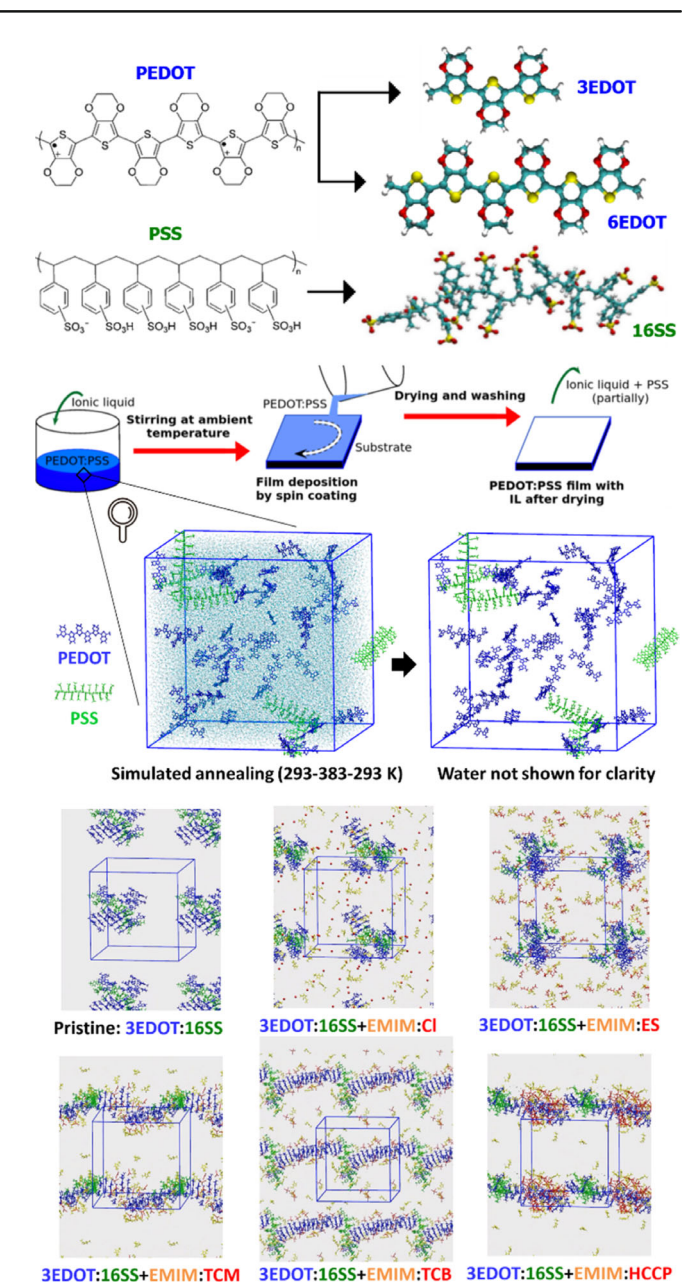


FIGURE 5 (Top) Larger models of PEDOT (3EDOT⁺ or 6EDOT²⁺; blue) and PSS (16SS¹⁶⁻; green) immersed in 6- or 12-nm-long periodic cubic boxes of water for MD simulations, whose final snapshots are mixed with ILs for further simulations. (Bottom) Final snapshots of MD simulations on the medium-size models of PEDOT:PSS mixed with EMIM:X (X = CI, ES, TCM, TCB, and HCCP; red) ILs. Adapted from references [52-55] (copyright ACS 2018, 2021, and 2023).

separation and PEDOT assembly are visible only with a sufficient amount of EMIM:TCM or EMIM:TCB, not with EMIM:CI or EMIM:ES (as also shown from the friendsof-friends analyses; Figure 6), owing to the ion exchange with soft anions in EMIM:TCM and EMIM:TCB ILs. The PSS chains, which were separated from PEDOT and pushed out of the extended π -stacked PEDOT domain, still remain near the surface of the PEDOT domain, but they would be washed away rather easily without disrupting the

LANSAC ET AL. BULLETIN OF THE 901

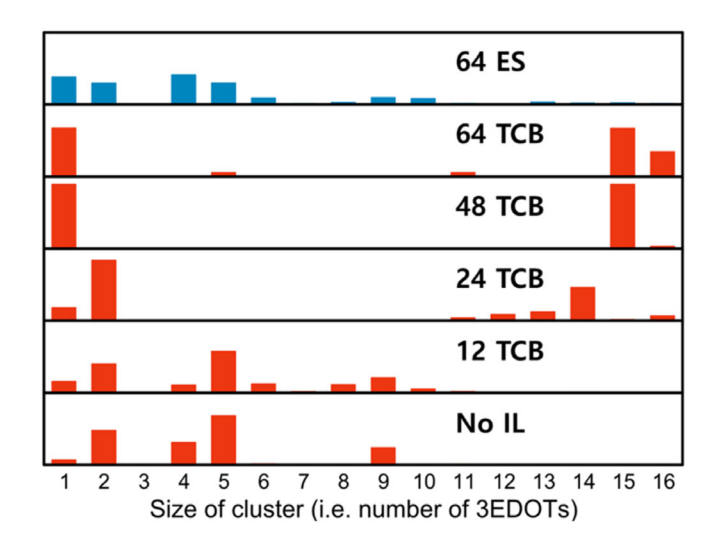


FIGURE 6 Friends-of-friends analysis (over the last 60-ns MD simulation shown in Figure 5) of the size of 3EDOT clusters formed after mixing with EMIM:ES (top; blue) or EMIM:TCB (bottom; red). PEDOT assembly into one large cluster (of size 16) is visible only with a sufficient amount of EMIM:TCB, not with EMIM:ES. Adapted from reference [52] (copyright ACS 2018).

formation of fibular PEDOT networks (as shown in Figure 2, bottom right).

New design: Protic-cation-soft-anion IL

According to the proposed hard-cation-soft-anion principle. the aromatic EMIM+ may not be the best cation for PEDOT:PSS treatment. Organic salts such as Inl₃, Li:TCB, and Li:TFSI [TFSI = $(CF_3SO_2)_2^-$] have induced high PEDOT:PSS conductivies, 47,90-95 and they are indeed combinations of soft anions (TCB⁻, TFSI⁻, and I⁻) and small or highlycharged, i.e., hard and hydrophilic metal cations (Li+ and In³⁺).⁶⁸ In fact, one of the smallest, the hardest, and the most hydrophilic cations is proton (H⁺). Indeed, treatments with concentrated acid H₂SO₄ or recent treatments with acids of rather hydrophobic conjugate bases (HI, CH₃SO₃H, or CF₃SO₃H) have achieved the highest conductivities of PEDOT:PSS so far (>4000 S cm⁻¹).^{29,32,40-44} A strong acid HI $(pK_a - 9.3)$ has been more effective than HCl. Films made at low pH have shown higher conductivity than those made at higher pH. Such treatment can be regarded as a process where the hardest cation H⁺ strongly interacts with PSS⁻ (even making a bond with it, i.e., protonating it to form PSSH) and leaves behind the soft anions for favorable interaction with PEDOT. Such a reasoning again supports the hard-cation-soft-anion IL design rule and leads us to propose new ILs, MIM:TCB or EIM:TCB, composed of a protic (and thus more hydrophilic and harder) derivative of EMIM⁺ cation, methyl or ethyl imidazolium (MIM⁺ or EIM⁺), and the most hydrophobic anion so far, TCB-, for PEDOT:PSS treatment, which was confirmed computationally and experimentally (Figure 7).55,56

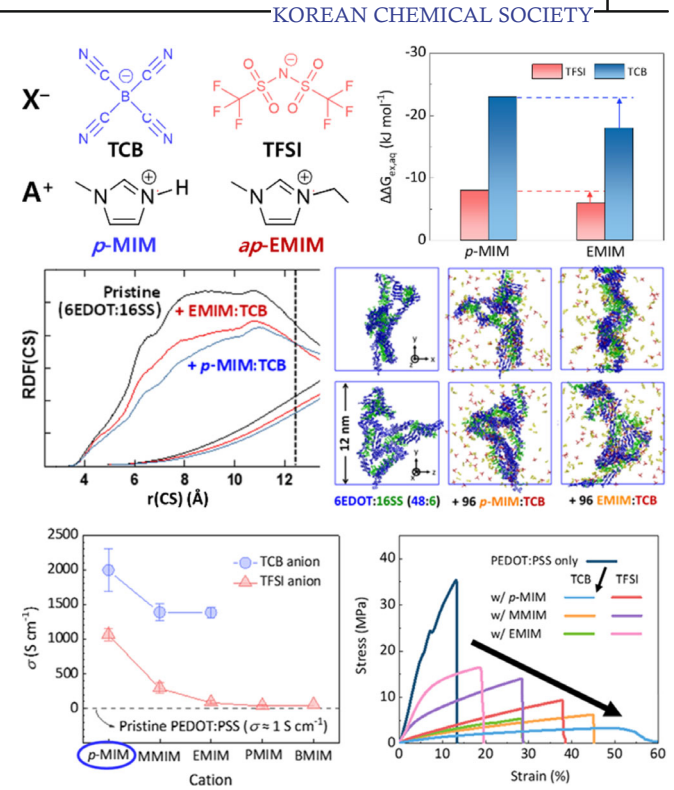


FIGURE 7 Protic ILs proposed according to the hard-cation-soft-anion design principle vs. aprotic ILs. (Top) Free energy of ion exchange with PEDOT:PSS (kJ mol $^{-1}$) estimated from DFT combined with the Poisson-Boltzmann implicit solvation model of water. (Middle) Final MD snapshots (viewed in two different directions) of pristine and IL-treated large model systems containing 48 chains of 6EDOT $^{2+}$ (blue) and 6 chains of 16 C(green) in each periodic cubic water box of 12 nm on each side and their radial distribution functions (RDF) between the sulfonate S atoms of 16SS and the backbone C atoms of 6EDOT before (black curve) and after mixing with EMIM:TCB (red curve) or MIM:TCB (blue curve). (Bottom) Conductivities and stress–strain curves of pristine or IL-treated 100-μm-thick PEDOT:PSS films. Adapted from reference [56] (copyright ACS 2023).

The aqueous-phase ion-exchange free energy $\Delta\Delta G_{\rm ex,aq}$ is estimated as -23 (MIM:TCB), -18 (EMIM:TCB), -6 (MIM:TFSI) and -4 (EMIM:TFSI) (kJ mol⁻¹, Figure 7, top) by DFT combined with the Poisson-Boltzmann implicit solvation model of water. More negative $\Delta \Delta G_{\text{ex.ag}}$ values indicate more favorable ion exchange. Indeed, the protic (thus more hydrophilic) MIM⁺ cation leads to a more favorable ion exchange than the aprotic EMIM⁺ (-23 < -18), most likely due to its strong H bond with PSS⁻ as shown by the short H-bond distance in the MIM:PSS ion pairs (2.85 Å for N-O). This cation effect is general (-6 < -4) when paired with another anion, bis(trifluoromethane)sulphonamide (TFSI⁻) but the most hydrophobic TCB⁻ anion still plays a key role in the ion exchange (-23 and -18 with TCB $^- << -6$ and -4 with TFSI⁻).⁵⁶

After mixing with the protic MIM:TCB, the whole 48 6EDOT units form a single stable cluster with \sim 55 (out of 96) sulfonate (SO $_3$ ⁻) groups of 16SS attached to it. On the contrary, the 48-unit 6EDOT cluster formed after

mixing with aprotic EMIM:TCB ILs (red curve).⁵⁶

As the first experimental confirmation of our firstprinciple-guided prediction, the PEDOT:PSS film treated with the protic MIM:TCB IL indeed shows the conductivity σ approaching 2500 S cm⁻¹, which is higher than the σ value achieved with the aprotic EMIM:TCB (Figure 7, bottom, blue dot). The generality of the cation effect over another anion (TFSI⁻) and the key role of the hydrophobic TCB⁻ is again confirmed (Figure 7, bottom, red dot).⁵⁶

IL-induced stretchability enhancement

The friend-of-friend analyses indicate that the phaseseparated PEDOT domains contain fewer IL components after being treated with MIM:TCB (\sim 60 TCB $^-$ and \sim 18 MIM⁺) than after being treated with EMIM:TCB (\sim 65 TCB⁻ and ~ 30 EMIM⁺).⁵⁶ Hydrophobic and planar EMIM⁺ cations appear to bind to (or even intercalate) the hydrophobic PEDOT domain and may adversely interfere with the separation of EMIM+:SO₃ pairs from the PEDOT domain and with the π -stacking (and/or electron transfer through the π -stacking) of PEDOT units in that domain. This adverse effect appears to be partially avoided by using hydrophilic MIM⁺ cations. However, a significant amount of planar MIM+ cations still remain around the PEDOT:TCB domains (via H bonds with TCB and π -stacking with PEDOT) while bonded to a significant (but not excessive) amount of PSS (via strong H bonds). Such protic-IL-mediated bridges (PEDOT:TCB-MIM:PSS-PEDOT: TCB) may hold multiple PEDOT domains together, enhancing the elastic property (stretchability) of the film as well as its conductivity. Indeed, significant increase in stretchability has been observed experimentally⁵⁶ after treating a PEDOT:PSS film with the protic MIM:TCB IL (Figure 7, bottom right, dark vs. light blue curves and Figure 8, i vs. ii). These IL-mediated bridges (TCB-MIM: PSS) are expected to reside on the outer surfaces of the PEDOT domains, since the radial distribution functions between PEDOT and PSS [RDF(C-S), Figure 7, middle left] show a crossover between the red (EMIM:TCB) and blue (MIM:TCB) curves around 12 Å. Then, these bridges (TCB-MIM:PSS) would be rather easily washed away from the PEDOT domains by excess water and acetonitrile, reducing the elasticity of the film, as confirmed experimentally (Figure 8, ii vs. iii-iv).⁵⁶ Then, most interestingly, when the MIM:TCB ILs are reintroduced to the film using a washing solvent containing them, the protic-IL-mediated bridges holding the multiple PEDOT domains (PEDOT:TCB-MIM: PSS-PEDOT:TCB) are restored with a much smaller

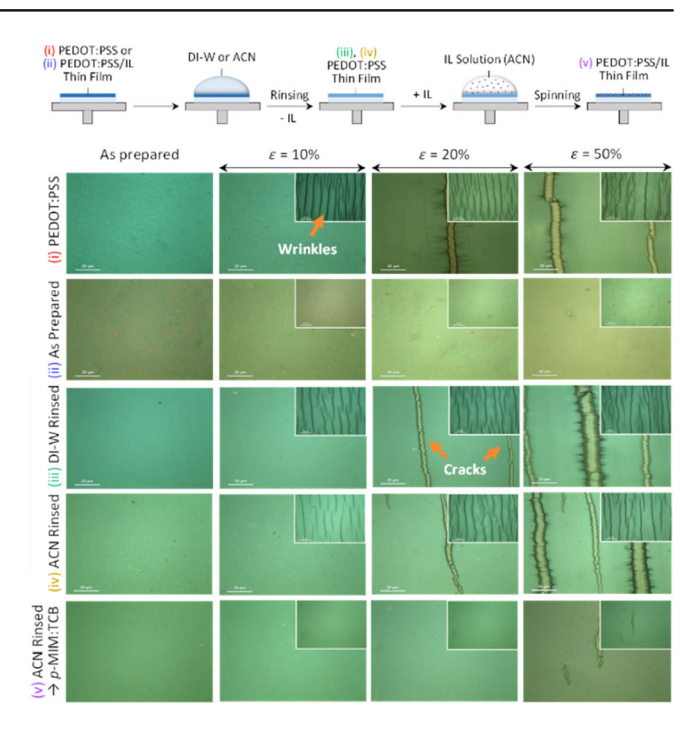


FIGURE 8 (Top) Various conditions of PEDOT:PSS film preparation (i to v). (Bottom) The corresponding (in each row; i to v) optical microscopy images obtained at various strain magnitudes (in each column; 0%-50%). The insets show the images of the thin films after the strain is removed. Adapted from reference [56] (copyright ACS 2023).

amount of PSS, achieving the enhancement of both conductivity and stretchability (Figure 8, iii-iv vs. v).⁵⁶ Uniaxial tensile-loading simulations mimicking the IL-induced stretchability improvement of PEDOT:PSS films are currently underway.

SUMMARY AND PERSPECTIVE

Combining our small-scale DFT calculations and large-scale MD simulations with various experiments performed in collaboration or found in literature, we have designed, predicted, and confirmed the improvement of both electrical (conductivity) and mechanical (stretchability) properties of PEDOT:PSS induced by hard-cation-soft-anion ILs, salts, and acids, such as (1) MIM:TCB IL, which is composed of protic MIM⁺ and hydrophobic TCB^{-,56} (2) Li:PFSI salt composed of small metal ion Li⁺, which is a point-like and thus hard and hydrophilic cation, and a bulky and hydrophobic PFSI⁻ anion, bis(pentafluoroethanesulfonyl)imide, which is bulkier than popular TFSI^{-,95} and (3) CF₃SO₃H acid, which is composed of the smallest (i.e., one of the hardest) cation H⁺ and a soft (at least softer than $SO_4^{2-})^{32,40}$ CF₃SO₃⁻ anion.²⁹ We have also proposed⁵⁵ PYR₃:TCB as promising IL (PYR₃ = 3-methyl pyrrolidinium = protic aliphatic cation) and PYR₁₃:TCB (PYR₁₃ = 1,3-dimethyl pyrrolidinium = nonprotic aliphatic cation)46,96 as less promising IL, although this proposition has not been experimentally confirmed. A non-protic but hydrophilic, aliphatic, and biocompatible

ditions) on Wiley Online Library for rules of use; OA articles are governed by the applicable Creative Commons

LANSAC ET AL.

BULLETIN OF THE 903

KOREAN CHEMICAL SOCIETY

tris(2-hydroxyethyl)-methylammonium cation can also be promising. 46,97

Various applications of PEDOT:PSS, ILs, and/or salts utilizing our ion-exchange-based design principle have been reported⁴⁶ for thermoelectrics, 95,98,99 Li-S batteries, 100 perovskite light emitting diodes, 101 organic solar cells, 102 and so on, or have a great potential to be introduced to many other areas such as liquid-phase exfoliation of two-dimensional materials 103 and electrolyte control for dendrite suppression in batteries. 104,105 Therefore, new force fields and protocols have been developed and utilized for MD and Monte Carlo (MC) simulations on various aspects of PEDOT:PSS and ILs. 106-110 We also plan to extend our work toward larger scale simulations on a coarse-grained model of PEDOT:PSS and ILs (as done for other polyelectrolytes such as DNA and peptide; see below)88,89 to estimate their electronic and ionic conductivities 109,110 quantitatively (beyond our previous qualitative estimation).52

Related to this plan, another extension of this line of our study is as follows. Although ionic PEDOT:PSS polymer is a polyelectrolyte with a tremendous industrial importance, nucleic acids such as DNA and RNA are polyelectrolytes with a tremendous biological importance. Just as PEDOT:PSS is composed of stiff PEDOT cations and flexible PSS anions, DNA is one of the longest and stiffest anions in nature, which is condensed into the tiny space of cell nuclei by various cationic small peptides. DNA is condensed even further during cell division or in sperm cells by a special cationic protein called protamine. Understanding the principles underlying such a fascinating and dynamic process between DNA or RNA and protamine would bring us one step closer not only to the origin of life but also to applications in various fields such as medicine, materials, and energy, but it is still difficult to observe such processes at the molecular level by real experiments. Hence, our studies on the IL-induced PEDOT:PSS phase change, which can be considered as a type of controlled liquidliquid phase separation, have a broad relevance to protein-controlled DNA packaging in vivo and in vitro as well as controlled packaging and depackaging of antiviral and anticancer mRNA vaccine platforms. Thus, as an immediate extension of our work on PEDOT:PSS, we perform molecular-level simulations on reversible condensation between DNA/RNA and protamine (or any other cationic peptides or polymers), 88,89,112,113 hoping for a clearer understanding of the mechanism involved in gene transfer or gene protection in the cell nuclei or in viruses, which will in turn accelerate the recent development of anticancer or antiviral mRNA vaccines.

PEDOT:PSS is also a conducting polymer, which will become a low-cost, light-weight, and flexible alternative (soft electronics) to the current silicon-based electronic device materials. Essentially an infinite number of chemical design is available to realize conducing polymers with desired electronic or optical properties. Thus, another

direction of extension of our current study would be a molecular-level understanding and rational design of electronic and optical properties of various conducting polymers. As an example, we design a *red-selective* polymer which can strongly absorb only the skin-penetrating visible light, i.e., the red light of wavelengths 625–800 nm, which is quite rare. Such a polymer will help realizing wireless and thus non-invasive power supply to subdermal bioelectronic implants (such as pacemaker on heart or neuromodulator on brain) by shedding the red light toward the red-light-absorbing organic photovoltaic thin film deposited on it. Such a polymer can also be used as a conformable RGB-color-selective photodiode component, which will help realizing retinal prosthesis and vision restoration. 114,115

ACKNOWLEDGMENTS

This work was supported by the National Research Foundation of Korea (RS-2024-00340218, 2019R1A2C2003118) and DGIST of Korea (24KUJoint10). The supercomputing time is supported by the KISTI Grand Challenge Program (KSC-2024-CRE-0287) and the DGIST Supercomputing Center.

FUNDING INFORMATION

NRF (RS-2024-00340218, 2019R1A2C2003118); DGIST (24KUJoint10); KISTI (KSC-2024-CRE-0287); DGIST Supercomputing Center.

ORCID

Yves Lansac https://orcid.org/0000-0002-3955-417X *Changwon Choi* https://orcid.org/0000-0003-4509-2909 *Yun Hee Jang* https://orcid.org/0000-0002-6604-5813

REFERENCES

- L. Jingcheng, V. S. Reddy, W. A. D. M. Jayathilaka, A. Chinnappan, S. Ramakrishna, R. Ghosh, *Polymer* 2021, *13*, 1427.
- [2] J. Bardeen, W. H. Brattain, Phys. Rev. 1948, 74, 230.
- [3] W. H. Brattain, J. Bardeen, Phys. Rev. 1948, 74, 231.
- [4] W. Shockley, G. L. Pearson, Phys. Rev. 1948, 74, 232.
- [5] Y.-Q. Zheng, Y. Liu, D. Zhong, S. Nikzad, S. Liu, Z. Yu, D. Liu, H. C. Wu, C. Zhu, J. Li, H. Tran, J. B. H. Tok, Z. Bao, Science 2021, 373, 88.
- [6] N. Matsuhisa, X. Chen, Z. Bao, T. Someya, Chem. Soc. Rev. 2019, 48, 2946.
- [7] W. Wang, Y. Jiang, D. Zhong, Z. Zhang, S. Choudhury, J. C. Lai, H. Gong, S. Niu, X. Yan, Y. Zheng, C. C. Shih, R. Ning, Q. Lin, D. Li, Y. H. Kim, J. Kim, Y. X. Wang, C. Zhao, C. Xu, X. Ji, Y. Nishio, H. Lyu, J. B. H. Tok, Z. Bao, *Science* 2023, 380, 735.
- [8] C. Zhao, J. Park, S. E. Root, Z. Bao, Nat. Rev. Bioeng. 2024, 2, 671.
- [9] P. Zhang, B. Zhu, P. Du, J. Travas-Sejdic, Chem. Rev. 2024, 124, 722.
- [10] R. M. Owens, G. G. Malliaras, MRS Bull. 2010, 35, 449.
- [11] E. Musk, Neuralink, J. Med. Internet Res. 2019, 21, e16194.
- [12] H. U. Chung, B. H. Kim, J. Y. Lee, J. Lee, Z. Xie, E. M. Ibler, K. H. Lee, A. Banks, J. Y. Jeong, J. Kim, C. Ogle, D. Grande, Y. Yu, H. Jang, P. Assem, D. Ryu, J. W. Kwak, M. Namkoong, J. B. Park, Y. Lee, D. H. Kim, A. Ryu, J. Jeong, K. You, B. Ji, Z. Liu, Q. Huo, X. Feng, Y. Deng, Y. Xu, K. I. Jang, J. Kim, Y. Zhang, R. Ghaffari, C. M. Rand, M. Schau, A. Hamvas, D. E. Weese-Mayer, Y. Huang, S. M. Lee, C. H. Lee, N. R. Shanbhag, A. S. Paller, S. Xu, J. A. Rogers, Science 2019, 363, eaau0780.

. 2295949, 2024, 11, Downloaded from https://onlinelibrary.wiley.com/doi/10.1002/bkcs.12908 by Daegu Gyeongbuk Institute Of, Wiley Online Library on [23/12/2024]. See the Term

of use; OA

articles are governed by the applicable Creative Commons

- [13] H. U. Chung, A. Y. Rwei, A. Hourlier-Fargette, S. Xu, K. H. Lee, E. C. Dunne, Z. Xie, C. Liu, A. Carlini, D. H. Kim, D. Ryu, E. Kulikova, J. Cao, I. C. Odland, K. B. Fields, B. Hopkins, A. Banks, C. Ogle, D. Grande, J. B. Park, J. Kim, M. Irie, H. Jang, J. H. Lee, Y. Park, J. Kim, H. H. Jo, H. Hahm, R. Avila, Y. Xu, M. Namkoong, J. W. Kwak, E. Suen, M. A. Paulus, R. J. Kim, B. V. Parsons, K. A. Human, S. S. Kim, M. Patel, W. Reuther, H. S. Kim, S. H. Lee, J. D. Leedle, Y. Yun, S. Rigali, T. Son, I. Jung, H. Arafa, V. R. Soundararajan, A. Ollech, A. Shukla, A. Bradley, M. Schau, C. M. Rand, L. E. Marsillio, Z. L. Harris, Y. Huang, A. Hamvas, A. S. Paller, D. E. Weese-Mayer, J. Y. Lee, J. A. Rogers, Nat. Med. 2020, 26, 418.
- [14] S. M. Won, L. Cai, P. Gutruf, J. A. Rogers, Nat. Biomed. Eng. 2023, 7, 405.
- [15] H. Shirakawa, E. J. Louis, A. G. MacDiarmid, C. K. Chiang, A. J. Heeger, J. Chem. Soc. Chem. Commun. 1977, 578.
- [16] G. Heywang, F. Jonas, Adv. Mater. 1992, 4, 116.
- [17] Q. Pei, G. Zuccarello, M. Ahlskog, O. Inganas, *Polymer* **1994**, *35*, 1347.
- [18] L. B. Groenendaal, F. Jonas, D. Freitag, H. Pielartzik, J. R. Reynolds, Adv. Mater. 2000, 12, 481.
- [19] F. Jonas, J. T. Morrison, Synth. Met. 1997, 85, 1397.
- [20] M. N. Gueye, A. Carella, J. Faure-Vincent, R. Demadrille, J.-P. Simonato, Prog. Mater. Sci. 2020, 108, 100616.
- [21] K. Sim, Z. Rao, F. Ershad, C. Yu, Adv. Mater. 2020, 32, 1902417.
- [22] J. Chang, A. Khot, B. M. Savoie, B. W. Boudouris, ACS Macro Lett. 2020, 9, 646.
- [23] J. Rivnay, S. Inal, A. Salleo, R. M. Owens, M. Berggren, G. G. Malliaras, Nat. Rev. Mater. 2018, 3, 17086.
- [24] S. H. Oh, J. Yoo, J. Lee, Macromol. Res. 2023, 31, 1189.
- [25] J. So, T. Kim, J. Shin, D. Kim, F. S. Kim, Macromol. Res. 2023, 31, 1095
- [26] L. Shen, Y. Ahn, Y. Kim, S. Kim, S. Choi, T.-D. Kim, D. Lee, *Macromol. Res.* 2024, 32, 767.
- [27] L. A. Fielding, J. K. Hillier, M. J. Burchell, S. P. Armes, Chem. Commun. 2015, 51, 16886.
- [28] Y. Li, R. Tanigawa, H. Okuzaki, Smart Mater. Struct. 2014, 23, 074010.
- [29] J. Park, J. G. Jang, K. Kang, S. H. Kim, J. Kwak, Adv. Sci. 2024, 11, 2308368.
- [30] T. Takano, H. Masunaga, A. Fujiwara, H. Okuzaki, T. Sasaki, Macromolecules 2012, 45, 3859.
- [31] Y. Honma, K. Itoh, H. Masunaga, A. Fujiwara, T. Nishizaki, S. Iguchi, T. Sasaki, Adv. Electron. Mater. 2018, 4, 1700490.
- [32] N. Kim, S. Kee, S. H. Lee, B. H. Lee, Y. H. Kahng, Y.-R. Jo, B.-J. Kim, K. Lee, Adv. Mater. 2014, 26, 2268.
- [33] C. M. Palumbiny, F. Liu, T. P. Russell, A. Hexemer, C. Wang, P. Müller-Buschbaum, Adv. Mater. 2015, 27, 3391.
- [34] Z. Fan, D. Du, Z. Yu, P. Li, Y. Xia, J. Ouyang, ACS Appl. Mater. Interfaces **2016**, *8*, 23204.
- [35] M. Modarresi, A. Mehandzhiyski, M. Fahlman, K. Tybrandt, I. Zozoulenko, *Macromolecules* 2020, 53, 6267.
- [36] M. Modarresi, J. F. Franco-Gonzalez, I. Zozoulenko, Phys. Chem. Chem. Phys. 2019, 21, 6699.
- [37] U. Lang, E. Müller, N. Naujoks, J. Dual, *Adv. Funct. Mater.* **2009**, *19*,
- [38] O. P. Dimitriev, Y. P. Piryatinski, A. A. Pud, J. Phys. Chem. B 2011, 115. 1357.
- [39] H. Yan, S. Arima, Y. Mori, T. Kagata, H. Sato, H. Okuzaki, *Thin Solid Films* 2009, 517, 3299.
- [40] S.-M. Kim, C. H. Kim, Y. Kim, N. Kim, W. J. Lee, E. H. Lee, D. Kim, S. Park, K. Lee, J. Rivnay, M. H. Yoon, Nat. Commun. 2018, 9, 3858.
- [41] Y. Xia, K. Sun, J. Ouyang, Adv. Mater. 2012, 24, 2436.
- [42] X. Wu, J. Liu, G. He, Org. Electron. 2015, 22, 160.
- [43] J. Ouyang, A. C. S. Appl, Mater. Interfaces 2013, 5, 13082.
- [44] A. K. Sarker, J. Kim, B.-H. Wee, H.-J. Song, Y. Lee, J.-D. Hong, C. Lee, RSC Adv. 2015, 5, 52019.
- [45] S. Chen, L. Song, Z. Tao, X. Shao, Y. Huang, Q. Cui, X. Guo, Org. Electron. 2014, 15, 3654.

- [46] Y. Li, Y. Pang, L. Wang, Q. Li, B. Liu, J. Li, S. Liu, Q. Zhao, Adv. Mater. 2024, 36, 2310973.
- [47] B. Wei, Z. Wang, H. Guo, F. Xie, S. Cheng, Z. Lou, C. Zhou, H. Ji, M. Zhang, X. Wang, X. Jiao, S. Ma, H. M. Cheng, X. Xu, Cell Rep. Phys. Sci. 2023, 4, 101335.
- [48] L. V. Lingstedt, M. Ghittorelli, H. Lu, D. A. Koutsouras, T. Marszalek, F. Torricelli, N. I. Crăciun, P. Gkoupidenis, P. W. M. Blom, Adv. Electron. Mater. 2019, 5, 1800804.
- [49] M. Modarresi, I. Zozoulenko, Phys. Chem. Chem. Phys. 2022, 24, 22073.
- [50] C. Badre, L. Marquant, A. M. Alsayed, L. A. Hough, Adv. Funct. Mater. 2012, 22, 2723.
- [51] S. Kee, N. Kim, B. S. Kim, S. Park, Y. H. Jang, S. H. Lee, J. Kim, J. Kim, S. Kwon, K. Lee, Adv. Mater. 2016, 28, 8625.
- [52] A. de Izarra, S. Park, J. Lee, Y. Lansac, Y. H. Jang, J. Am. Chem. Soc. 2018, 140, 5375.
- [53] A. de Izarra, C. Choi, Y. H. Jang, Y. Lansac, J. Phys. Chem. B 1916, 2021, 125.
- [54] A. de Izarra, C. Choi, Y. H. Jang, Y. Lansac, J. Phys. Chem. B 2021, 125, 8601.
- [55] C. Choi, A. de Izarra, I. Han, W. Jeon, Y. Lansac, Y. H. Jang, J. Phys. Chem. B 2022, 126, 1615.
- [56] M. Kim, S. Y. Lee, J. Kim, C. Choi, Y. Lansac, H. Ahn, S. Park, Y. H. Jang, S. H. Lee, B. H. Lee, ACS Appl. Mater. Interfaces 2023, 15, 3202.
- [57] G. Zotti, S. Zecchin, G. Schiavon, F. Louwet, L. Groenendaal, X. Crispin, W. Osikowicz, W. Salaneck, M. Fahlman, *Macromolecules* 2003, 36, 3337.
- [58] P. K. Kahol, J. C. Ho, Y. Y. Chen, C. R. Wang, S. Neeleshwar, C. B. Tsai, B. Wessling, Synth. Met. 2005, 151, 65.
- [59] S. Kirchmeyer, K. Reuter, J. Mater. Chem. 2005, 15, 2077.
- [60] D. Kim, I. Zozoulenko, J. Phys. Chem. B 2019, 123, 5160.
- [61] B. H. Greeley, T. V. Russo, D. T. Mainz, R. A. Friesner, J. M. Langlois, W. A. Goddard, R. E. Donnelly, M. N. Ringnalda, J. Chem. Phys. 1994, 101, 4028.
- [62] A. D. Bochevarov, E. Harder, T. F. Hughes, J. R. Greenwood, D. A. Braden, D. M. Philipp, D. Rinaldo, M. D. Halls, J. Zhang, R. A. Friesner, Int. J. Quantum Chem. 2013, 113, 2110.
- [63] G. M. Torrie, J. P. Valleau, J. Comput. Phys. 1977, 23, 187.
- [64] B. Marten, K. Kim, C. Cortis, R. A. Friesner, R. B. Murphy, M. N. Ringnalda, D. Sitkoff, B. Honig, J. Phys. Chem. 1996, 100, 11775.
- [65] D. J. Tannor, B. Marten, R. Murphy, R. A. Friesner, D. Sitkoff, A. Nicholls, M. Ringnalda, W. A. Goddard III, B. Honig, J. Am. Chem. Soc. 1994, 116, 11875.
- [66] R. G. Pearson, J. Am. Chem. Soc. 1963, 85, 3533.
- [67] G. Klopman, J. Am. Chem. Soc. 1968, 90, 223.
- [68] R. G. Pearson, J. Chem. Educ. 1968, 45, 581.
- [69] R. G. Pearson, J. Chem. Educ. 1968, 45, 643.
- [70] H. J. C. Berendsen, J. R. Grigera, T. P. Straatsma, J. Phys. Chem. 1987, 91, 6269.
- [71] W. L. Jorgensen, J. Tirado-Rives, Proc. Natl. Acad. Sci. 2005, 102, 6665.
- [72] G. A. Kaminski, R. A. Friesner, J. Tirado-Rives, W. L. Jorgensen, J. Phys. Chem. B 2001, 105, 6474.
- [73] W. L. Jorgensen, D. S. Maxwell, J. Tirado-Rives, J. Am. Chem. Soc. 1996, 118, 11225.
- [74] J. F. Franco-Gonzalez, I. V. Zozoulenko, J. Phys. Chem. B 2017, 121, 4299.
- [75] T. Sedghamiz, A. Y. Mehandzhiyski, M. Modarresi, M. Linares, I. Zozoulenko, Chem. Mater. 2023, 35, 5512.
- [76] U. Essmann, L. Perera, M. L. Berkowitz, T. Darden, H. Lee, L. G. Pedersen, J. Chem. Phys. 1995, 103, 8577.
- [77] T. Darden, D. York, L. Pedersen, J. Chem. Phys. 1993, 98, 10089.
- [78] H. J. C. Berendsen, D. van der Spoel, R. van Drunen, Comput. Phys. Commun. 1995, 91, 43.
- [79] B. Hess, C. Kutzner, D. van der Spoel, E. Lindahl, J. Chem. Theory Comput. 2008, 4, 435.

onditions) on Wiley Online Library for rules of use; OA articles are governed by the applicable Creative

LANSAC ET AL.

BULLETIN OF THE

KOREAN CHEMICAL SOCIETY

SOURCE

BULLETIN OF THE

BULLETIN OF THE

SOURCE

FOR EACH CHEMICAL SOCIETY

- [80] H. J. C. Berendsen, J. P. M. Postma, W. F. van Gunsteren, A. DiNola, J. R. Haak, J. Chem. Phys. 1984, 81, 3684.
- [81] S. Nosé, J. Chem. Phys. 1984, 81, 511.
- [82] W. G. Hoover, Phys. Rev. A 1985, 31, 1695.
- [83] S. Nosé, M. L. Klein, Mol. Phys. 1983, 50, 1055.
- [84] M. Parrinello, A. Rahman, J. Appl. Phys. 1981, 52, 7182.
- [85] R. W. Hockney, J. W. Eastwood, Computer Simulations Using Particles, McGraw-Hill, New York 1981.
- [86] Y. C. Kwon, D. Nunley, J. P. Gardner, M. Balazinska, B. Howe, S. Loebman, in *Scientific and Statistical Database Management* (Ed: G. M. B. Ludäscher), Springer-Verlag, Berlin Heidelberg **2010**, p. 132.
- [87] Y. Lansac, J. Degrouard, M. Renouard, A. C. Toma, F. Livolant, E. Raspaud, Sci. Rep. 2016, 6, 21995.
- [88] A. Mukherjee, A. de Izarra, J. Degrouard, E. Olive, P. K. Maiti, Y. H. Jang, Y. Lansac, ACS Nano 2021, 15, 13094.
- [89] Y. H. Jang, E. Raspaud, Y. Lansac, Nanoscale Adv. 2023, 5, 4798.
- [90] Y. Xia, J. Ouyang, Org. Electron. 2010, 11, 1129.
- [91] T. Kuppers, E. Bernhardt, H. Willner, H. W. Rohm, M. Kockerling, Inorg. Chem. 2005, 44, 1015.
- [92] Y. Wang, C. Zhu, R. Pfattner, H. Yan, L. Jin, S. Chen, F. Molina-Lopez, F. Lissel, J. Liu, N. I. Rabiah, Z. Chen, J. W. Chung, C. Linder, M. F. Toney, B. Murmann, Z. Bao, Sci. Adv. 2017, 3, e1602076.
- [93] Q. Li, M. Deng, S. Zhang, D. Zhao, Q. Jiang, C. Guo, Q. Zhou, W. Liu, J. Mater. Chem. C 2019, 7, 4374.
- [94] X. Li, Z. Liu, Z. Zhou, H. Gao, G. Liang, D. Rauber, C. W. M. Kay, P. Zhang, ACS Appl Polym. Mater. 2021, 3, 98.
- [95] Q. Li, Q. Zhou, W. Xu, L. Wen, J. Li, B. Deng, J. Zhang, H. Xu, W. Liu, A. C. S. Appl, *Mater. Interfaces* **2022**, *14*, 27911.
- [96] R. del Olmo, T. C. Mendes, M. Forsyth, N. Casado, J. Mater. Chem. A 2022, 10, 19777.
- [97] T. Li, J. Y. Cheryl Koh, A. Moudgil, H. Cao, X. Wu, S. Chen, K. Hou, A. Surendran, M. Stephen, C. Tang, C. Wang, Q. J. Wang, C. Y. Tay, W. L. Leong, ACS Nano 2022, 16, 12049.
- [98] J. Wang, Q. Li, K. Li, X. Sun, Y. Wang, T. Zhuang, J. Yan, H. Wang, Adv. Mater. 2022, 34, 2109904.
- [99] Y. Zhou, C. Yao, X. Lin, J. Oh, J. Tian, W. Yang, Y. He, Y. Ma, K. Yang, B. Ai, K. Sun, Z. Fu, Y. Lu, F. Li, C. Yang, S. Chen, *Adv. Funct. Mater.* 2023, 33, 2214563.
- [100] D. Son, H. Park, W. G. Lim, S. Baek, S. H. Kang, J. C. Lee, T. Maiyalagan, Y. G. Lee, S. Park, J. Lee, ACS Nano 2023, 17, 25507.
- [101] M.-S. Kim, P. Sadhukhan, J.-M. Myoung, Adv. Funct. Mater. 2024, 34, 2309436.
- [102] C. Hou, H. Yu, J. Mater. Chem. C 2020, 8, 4169.
- [103] Y. Jeong, P. Samorì, Bull. Korean Chem. Soc. 2024, 45, 110.
- [104] H. Ham, G. Sim, W. Choi, M. J. Park, Bull. Korean Chem. Soc. 2024, 45, 200.
- [105] M. Lim, J. Lee, S. Lee, S. Park, H. Lee, Bull. Korean Chem. Soc. 2024, 45, 648.
- [106] W. Michaels, Y. Zhao, J. Qin, Macromolecules 2021, 54, 3634.
- [107] W. Michaels, Y. Zhao, J. Qin, Macromolecules 2021, 54, 5354.
- [108] H. Makki, A. Troisi, J. Mater. Chem. C 2022, 10, 16126.
- [109] H. Lim, Y. Jung, Bull. Korean Chem. Soc. 2022, 43, 626.
- [110] H. Park, C. B. Park, B. J. Sung, Bull. Korean Chem. Soc. 2023, 44, 736.
- [111] S. Bag, P. K. Maiti, Phys. Chem. Chem. Phys. 2019, 21, 23514.
- [112] A. Mukherjee, S. Saurabh, E. Olive, Y. H. Jang, Y. Lansac, J. Phys. Chem. B 2021, 125, 3032.

- [113] K. B. Chhetri, Y. H. Jang, Y. Lansac, P. K. Maiti, Biophys. J. 2022, 121, 4830.
- [114] C. Choi, W. Jeon, Y. Lansac, Y. H. Jang, J. Phys. Chem. C 2022, 126, 12230.
- [115] W. Jeon, C. Choi, J. Cheon, J. Lee, Y. Lansac, Y. H. Jang, J. Phys. Chem. C 2023, 127, 15290.

AUTHOR BIOGRAPHIES

Yves Lansac received B.S. in Physics-Methematics (1985) and Ph.D. in Condensed Matter Physics (1993) from University of Nice, France. After working as post-doctoral scholar at University of Colorado, Boulder and as research staff at Caltech (USA), since 2004, he has been professor of CNRS and Department of Physics, University of Tours, France. His research involves the application of computer simulation and numerical modeling to the study of equilibrium and non-equilibrium self-organization in soft matter systems such as liquid crystals, colloids, and biomaterials.

Changwon Choi received his B.S. degree from DGIST, Daegu, Korea in 2018. He is currently pursuing a Ph.D. degree in Energy Science and Engineering under the supervision of Prof. Yun Hee Jang and Prof. Yves Lansac at DGIST. His main research interest is a molecular modeling of organic electronics materials, devices, and processes.

Yun Hee Jang received B.S. in Chemistry (1990) and Ph.D. in Physical Chemistry (1995) from Seoul National University (Seoul, Korea). After working as postdoctoral scholar at Caltech (USA) and as assistant and associate professor of Materials Science & Engineering at GIST (Gwangju, Korea), since 2016, she has been professor of Energy Science & Engineering in DGIST (Daegu, Korea). Her Curious Minds' Molecular Modeling (CMMM) group uses molecular-modeling and computational-chemistry tools for molecular-level understanding of structures and functions of various materials at interfaces.

How to cite this article: Y. Lansac, C. Choi, Y. H. Jang, *Bull. Korean Chem. Soc.* **2024**, *45*(11), 896. https://doi.org/10.1002/bkcs.12908